Article:

eprints@whiterose.ac.uk
https://eprints.whiterose.ac.uk/

Single grain K-feldspar MET-IRSL sediment transport determination: bleaching patterns and rates

Rhodes, E.J.[1], Spano, T.C.M.[1], Hodge, R.A.[2], Sawakuchi., A.O.[3], Bertassoli, D.J. Jr[3].

1 School of Geography and Planning, The University of Sheffield, Sheffield, S10 2TN, United Kingdom

2 Department of Geography, Durham University, Durham, DH1 3LE, United Kingdom

3 Institute of Geosciences, University of São Paulo, Rua do Lago, 562, São Paulo, SP, Brazil, 05508-080

Abstract

This paper describes ways that Infra-Red Stimulated Luminescence (IRSL) signals from K-feldspar grains can be used to determine patterns and rates of sediment transport. In particular, it focusses on the potential provided by single grains to reveal their individual exposure and burial histories by the application of multiple elevated temperature (MET) IRSL measurements. We examine similarities and differences in bleaching behaviour with different light sources and introduce the concept of an equilibrium bleach. We present data on the variability of bleaching parameters for grains from single sediment samples, and discuss different analysis approaches to best determine individual grain histories. We describe a single grain "bleach recovery" experiment, and the application of a combined growth-bleach protocol designed to allow optimal data collection of both aspects of grain behaviour. We discuss the development of a burial-bleach model using numerical simulations based on direct observations of sample characteristics.

1. Introduction

As sediment travels through the environment, grains and clasts experience periods of burial, during which the trapped charge populations that give rise to luminescence signals grow. These are interspersed with periods of transport when grains and clasts may be exposed to daylight; in this case, light-sensitive components of the trapped charge population can be reduced as charge is evicted. This process is referred to as bleaching, and when this occurs to a significant degree it is also called signal zeroing. In many cases, exposure duration is insufficient to remove some components of the light-sensitive trapped charge population; this

conditions is referred to as incomplete or partial bleaching (or zeroing). Where the primary aim of a particular research project is to undertake luminescence dating of sediment, incomplete bleaching prior to deposition can represent a problem that may lead to age overestimation if this condition is not detected.

Multiple Elevated Temperature IRSL (Infra-Red Stimulated Luminescence; Li and Li, 2011) provides the opportunity to measure several signals with different characteristic bleaching rates in a single sample or single grain (Fu and Li, 2013). Apparent ages can be determined for each signal, and concordance between different temperature components can be used as evidence of full bleaching (e.g. Reimann et al., 2015) besides reflecting thermal stability.

In this paper we briefly describe different luminescence approaches that have been used to help determine how sediment is transported through the environment, and examine how MET-IRSL signals from single grains can be used to elucidate transport rates and patterns. We present new data for MET-IRSL bleaching at different wavelengths and explore differences between feldspar samples with different chemical composition. Results from a single grain bleach recovery experiment are used to compare different approaches to track the different burial and bleach histories of individual feldspar grains.

2. State of the Art

2.1. Multiple Elevated Temperature IRSL

Previous research into IRSL signals of feldspar suggest that these are different in several substantive ways from quartz OSL, providing some additional opportunities, and also some issues that require care. Perhaps the clearest difference in both TL and optical determinations (OSL and IRSL) was the lack of well-defined first order signals in feldspar, leading to the concept of the "continuum" (e.g. Sanderson, 1988). Subsequent research suggests that this was caused not by a range of trap depths, but rather by restrictions in charge reaching luminescence centres via quantum mechanical tunnelling (Huntley and Lamothe, 2001; Huntley, 2006). Jain and Ankaerjaard (2011) clarified details of the recombination pathways, including the suggestion of Poolton et al. (2002) that band tail states played a significant role, with a simple power law decay model for IRSL developed by Pagonis et al. (2012). Guerin and Visocekas (2015) suggested that electron hopping may also contribute to anomalous fading observed in volcanic feldspar samples, where both thermal and non-thermal components were observed.

It seems likely to the present authors that MET-IRSL "signals" may represent electrons coming from one (or a small number of) trap type(s), but with both ambient temperature

bleaching and raised temperature IRSL sampling this same recombination continuum related to electron transport distance within the lattice. In this view, higher temperature MET-IRSL measurements primarily speed up the recombination of what would be a single long bleaching tail at a lower temperature. In other words, the researcher imposes a pre-selected set of measurement conditions that allow for the efficient reading of populations of electrons from less bleachable locations at higher temperatures; the less bleachable charge comes from electron traps that happen not to have luminescence centres located close by, so the probability of recombination at a given temperature during bleaching is reduced. However, we note that it is often convenient to discuss these as though they were discrete signals, and we have not ruled out the possibility that this is the case.

2.2 Sediment transport determination

Information concerning patterns and rates of sediment transport and storage can be determined using changes in the trapped charge populations responsible for luminescence signals of mineral grains, including TL (thermoluminescence), OSL (optically stimulated luminescence) and IRSL (Infra-Red Stimulated Luminescence). Trapped charge concentration can decrease by optical bleaching (light exposure), and grow during burial in response to natural environmental radiation. The concept of tracing fluvial sediment transfer, and studying spatial and temporal variations in residual signals, were the motivations for luminescence measurements by Gemmel (1985; 1988), Stokes (1992), Stokes et al. (2001) and Colls et al. (2001). Kars et al. (2014) provide an overview to that point of feldspar IRSL bleaching and its relationship to dating studies. McGuire and Rhodes (2015a) demonstrated how MET-IRSL could be used to determine virtual velocities (downstream transport velocity of sediment) using conventional multiple grain (MG) aliquots, developing a numerical model based on time and space equivalency principles; subsequently they also showed how single grain MET-IRSL could be used to test assumptions required for the application of this model, finding these conditions to be sustained in the case of the Mojave River (McGuire and Rhodes, 2015b). A more sophisticated model that incorporated specific consideration of different bleaching opportunities (during fluvial transport besides while grains are exposed at the surface of sediment bars) specifically designed to interface with hydrological sediment transfer models more easily was developed by Gray et al. (2017), and applied to a range of different rivers using a post-IR IRSL approach with conventional MG aliquots (Gray et al., 2018). Gray et al. (2019) provide a useful review of the topic.

Using post-IR IRSL measurements based on single grains of feldspar, Guyez et al. (2023) developed a different modelling approach, matching the changes in the mean values of three

IRSL parameters downstream in two large New Zealand rivers; they also used a time-space equivalency approach, combining single grain results to determine the average change in i) mean equivalent dose (D_e), ii) proportion of bleached grains, and iii) proportion of saturated grains.

2.3 Single grain bleaching

The use of single grains of alkali feldspar with a MET-IRSL approach can in principle recover similar, though less detailed, bleach duration information as that acquired from a single signal rock slice profile measurement suite (i.e. signal vs depth; Guralnik and Sohbati, 2019). For single grains, the different MET-IRSL signals, measured at increasing temperatures, behave with respect to optical bleaching in a manner analogous to rock slices at increasing depth, with the deeper and higher temperature IRSL signals bleaching more slowly than those from shallower depths or measured at lower temperatures (Fig. 1).
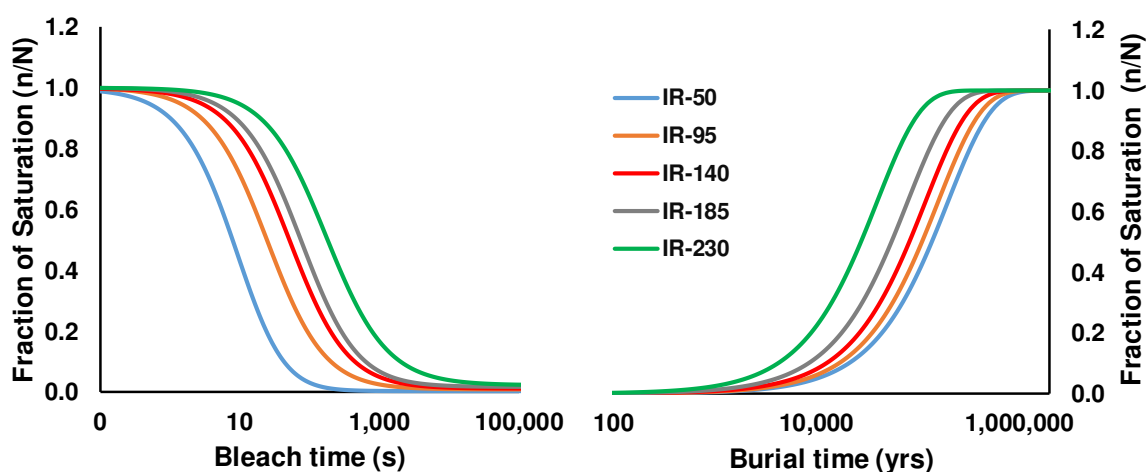
Figure 1. Model displaying the bleaching by light and subsequent growth to saturation during burial for five MET-IRSL signals from K-feldspar. Model data are based on grains from the Mojave River, California, USA. The numbers in the key refer to the measurement temperature in °C for each signal. N represents the number of traps available, n the number occupied. Note the different timescales (seconds, years), plotted using logarithmic axes.

Rhodes and Leathard (2022) provide an initial assessment of the utility of both storage time determination and also information relating to exposure duration using single grain MET-IRSL data. This included a comparison of "plateau ages" (where multiple MET-IRSL signals provide indistinguishable apparent age determinations) for glacial sediments from Derbyshire, United Kingdom, which were in agreement with independent chronological control, and also two novel single grain parameters that depend on bleaching duration. These parameters are "bleaching index" based on the "depth" of individual plateaus in terms of bleach duration, and the more complex "burial-bleach ratio" (B-B ratio). This latter parameter, which has a relationship to mean repeated burial duration and exposure period, can provide an assessment that extends over multiple burial and bleaching cycles, and was shown to have a close relationship to sedimentological characteristics represented by particle size analysis (PSA) for a suite of different samples (Rhodes and Leathard, 2022). In principle, the B-B ratio contains information about average burial and exposure times, as witnessed by that individual grain over several cycles since a previous "resetting" either by light (reduction of trapped charge populations to zero) or by extended burial producing saturation (filling of all participating traps).

This paper focusses on bleaching in the laboratory and natural settings and its relevance to application of MET-IRSL for reconstructing sediment transport rates and patterns.

3. Methods

3.1 IRSL measurement

Measurements were made with an unmodified Risø TL-DA-20 CD DASH luminescence reader using BG3 & BG39 (Risø blue filter pack) for all IRSL measurements, and 7.5mm of Hoya U340 filter when samples were exposed to blue or green LEDs within the reader. The instrument uses an Electron Tube 1" EMD-9107 PMT (photomultiplier tube), and clusters of stimulation LEDs at different wavelengths, namely blue (two clusters of Epitex SMBB470-1100-TINA-RS), green (two clusters of SMBB525-1100-TINA-RS), and IR (three clusters of SMBB870-1100-TINA-RS; see Lapp et al., 2015 for further details). Single grain IRSL stimulation was performed using a 150 mW 830 nm IR laser passed through a single RG-780 filter to reduce the resonance emission at 415 nm.

We performed three types of IRSL measurement, namely i) conventional multiple grain (MG) IRSL using a MET approach, ii) short-shine MG IRSL at 50°C, and iii) single grain MET-IRSL using several different protocols. Table 1 shows different SAR protocols as constructed for

single grain measurements, with 2.5s IR laser exposure times. In single grain SAR determinations, the IRSL signal used was the first 0.5s minus a background from the last 0.5s of the 2.5s laser exposure. For MG SAR, the main IRSL measurements at different elevated temperatures exposures were performed for 24s; other steps such as hot bleach treatments were unchanged.

Short shine IRSL measurements at 50°C were used to explore how different dose and bleaching treatments modify the decay rate and form of this signal. Using this technique can be efficient, as each brief IRSL measurement is designed to have very little impact on the trapped charge population. In this manner, a single dose and preheat can be given to an aliquot, and then the bleaching of the IR_{50} signal by another light source (e.g. blue diodes) can be made by alternating between IR_{50} short shine and bleach treatments. Correction for signal reduction from the IR measurements can be made simply by repeating the protocol without the bleach treatments, retaining only the IR_{50} short shine measurements; these values can be used to correct the signal loss of the bleaching experiment data (I_B) at each step by multiplying the IR_{50} signal at time t, (I_{Bt}), by I_{C0}/I_{Ct} of the correction data (I_C). In these experiments, a short shine of 0.1s at 90% power with the IRSL diodes was used; protocol is shown in table S1 (Supplementary Information).

Building on the approach developed by McGuire and Rhodes (2015a, b), a five step MET-IRSL procedure was used in some instances (Table 1, third column). Recent and ongoing measurements use a MET protocol we term METx which also contains a larger test dose and a "warm bleach" before the test dose, conceptually similar to the final "hot bleach" SAR step (Table 1, fourth column); these changes were introduced in an attempt to achieve improved growth characteristics, specifically exponential growth in contrast to exponential plus linear patterns regularly observed with our original five temperature protocol (MET-IRSL); changes followed the valuable findings and advice of Colarossi et al. (2018). The preheat used for both was the same as that used in the post-IR IRSL at 225°C protocol often applied in our laboratory for dating sediments (e.g. Rhodes, 2015; Rhodes and Walker, 2018; Zinke et al., 2017; Table 1 first column). This provided some degree of consistency, enabled comparison and helped with predicting loss on bleaching, for example.

Table 1. Details of single grain SAR protocols used or referred to in the text. IRSL measurements are shown in bold text. MG means that all grains were bleached at the same time using IR LEDS mounted in the DASH Risø reader for that step. Additional bleach treatments were performed in some experiments at 51°C between steps 1 and 2; see text for further details.

post-IR-IRSL$_{225}$ protocol	ILT-3ET protocol	MET-IRSL protocol	METx protocol
1) Natural or laboratory beta dose	1) Natural or laboratory beta dose	1) Natural or laboratory beta dose	1) Natural or laboratory beta dose
2) Preheat 60s 250°C 5°Cs^{-1}	2) Preheat 60s 170°C 5°Cs^{-1}	2) Preheat 60s 250°C 5°Cs^{-1}	2) Preheat 60s 250°C 5°Cs^{-1}
3) **SG IRSL 50°C 2.5s 90% power**	3) **SG IRSL 50°C 2.5s 90% power**	3) **SG IRSL 50°C 2.5s 90% power**	3) **SG IRSL 50°C 2.5s 90% power**
	4) **SG IRSL 95°C 2.5s 90% power**	4) **SG IRSL 95°C 2.5s 90% power**	4) **SG IRSL 95°C 2.5s 90% power**
	5) **SG IRSL 140°C 2.5s 90% power**	5) **SG IRSL 140°C 2.5s 90% power**	5) **SG IRSL 140°C 2.5s 90% power**
		6) **SG IRSL 185°C 2.5s 90% power**	6) **SG IRSL 185°C 2.5s 90% power**
4) **SG IRSL 225°C 2.5s 90% power**		7) **SG IRSL 230°C 2.5s 90% power**	7) **SG IRSL 230°C 2.5s 90% power**
	6) MG IRSL Warm Bleach 160°C 400s 90%		8) MG IRSL Warm Bleach 250°C 200s 90%
5) Beta test dose 8 Gy	7) Beta test dose 20 Gy	8) Beta test dose 8 Gy	9) Beta test dose 20 Gy
6) Preheat 60s 250°C 5°Cs^{-1}	8) Preheat 60s 170°C 5°Cs^{-1}	9) Preheat 60s 250°C 5°Cs^{-1}	10) Preheat 60s 250°C 5°Cs^{-1}
7) **SG IRSL 50°C 2.5s 90% power**	9) **SG IRSL 50°C 2.5s 90% power**	10) **SG IRSL 50°C 2.5s 90% power**	11) **SG IRSL 50°C 2.5s 90% power**
	10) **SG IRSL 95°C 2.5s 90% power**	11) **SG IRSL 95°C 2.5s 90% power**	12) **SG IRSL 95°C 2.5s 90% power**
	11) **SG IRSL 140°C 2.5s 90% power**	12) **SG IRSL 140°C 2.5s 90% power**	13) **SG IRSL 140°C 2.5s 90% power**
		13) **SG IRSL 185°C 2.5s 90% power**	14) **SG IRSL 185°C 2.5s 90% power**
8) **SG IRSL 225°C 2.5s 90% power**		14) **SG IRSL 230°C 2.5s 90% power**	15) **SG IRSL 230°C 2.5s 90% power**
9) MG IRSL Hot Bleach 290°C 100s 90%	12) MG IRSL Hot Bleach 180°C 400s 90%	15) MG IRSL Hot Bleach 290°C 100s 90%	16) MG IRSL Hot Bleach 290°C 100s 90%

As well as the five step MET-IRSL and METx protocols, a three elevated temperature (3ET) single grain protocol (Table 1, second column) conceptually similar to that developed for dating sediments (Ivester et al., 2022) was explored. The original 3ET approach used the same preheat as that of post-IR IRSL$_{225}$ of 250°C for 60s; for some applications we aim to explore burial periods of decades or less, so the preheat temperature was reduced to 170°C, allowing us to retain the first three MET-IRSL measurement temperatures of 50, 95 and 140°C. This protocol, termed ILT (Improved Low Temperature) 3ET, also incorporates a warm bleach before the test dose. Some of the advantages of using a lower preheat temperature can be understood from the data presented by Zhang et al. (2023).

In some experiments conventional MG discs were used. Grains were arranged centrally on 1cm aluminium discs in a smaller disc of diameter ~6mm. These were adhered using RS 60,000 viscosity silicone oil, subsequently covered in spray acrylic and allowed to dry. When MG discs were used in SAR protocols, IRSL measurement time was increased from 2.5s for SG to 24s, also at 90% power.

3.2 Experimental design

As part of our efforts to model the bleaching and growth of signals accurately, we have designed experiments to explore how the form of bleach response decay as well as the decay rate change in response to bleaching by different light sources. We also explore how chemical composition, the size of the dose used, and the effects of incomplete bleaching affect these decay parameters. Note, we have not explored changes in the shape of

individual IRSL shine-down curves; for single grain measurements, we consider that these may represent an unreliable guide to internal lattice and charge effects, as many external factors such as shielding can affect light intensity.

To study bleach form and rate dependency on the wavelength of bleaching light we constructed several MG aliquots from laboratory standard samples. To illustrate the effects on K feldspar, we used an orthoclase sample called MJ39 (Lawson et al. 2015; Daniels, 2016). The sample was previously prepared in daylight, so aliquots were first bleached for one hour in bright sunshine, followed by a METx hot bleach (290°C IRSL for 100s) and given a dose of ~144Gy. The METx protocol for MG discs was applied (Table 1, MET-IRSL measurements adjusted to 24s with 90% diode illumination, signal used was 0-4.5s minus a background based on 19.5-24.0s) for the unbleached signal; in subsequent cycles, following the same beta dose, either blue, green or IR diodes (51°C, 90% power) were used with exposure times of 1, 10, 100, 1000 and 10,000s followed by the preheat and subsequent SAR steps. The data were corrected for any sensitivity change in the same manner as for dating using the test dose responses with the same time integrals.

In order to investigate bleaching dependence on feldspar composition, similar discs of a bytownite (plagioclase) lab standard (MJ40) were made, and treated in an identical fashion to the procedure described above.

In order to explore bleach form and rate dependency on the size of dose, discs of different laboratory standard samples, MJ39, MJ40 and an orthoclase related to the Lowe Intrusion in the San Gabriel Mountains, California (lab code 22094) were constructed. Again, each aliquot was exposed to natural sunlight and given the METx-IRSL hot bleach. In a series of METx-SAR cycles, each aliquot was given doses of 8, 34, 144 and 480Gy, and the full IRSL signals at each METx temperature recorded and sensitivity corrected. Short shine IRSL measurements of just the IR_{50} signal at different doses were also used, to explore this more rapid means of assessing sample dependence on prior dose.

Short shine MG IR_{50} signal measurements were also used to explore and illustrate bleach form and rate dependency on previous bleaching, an important effect in the modelling of IRSL growth and reduction in natural environments. Following signal resetting using a METx hot bleach, these used a dose of 8Gy, a preheat of 170°C for 60s, then 0.1s IR_{50} short shines (at 90% power) alternating with blue LED exposures of 1.0s (90% power, 50°C) for 20 cycles. The procedure was repeated starting with a hot bleach, but this time with an initial 10s blue OSL bleach included after the 8 Gy dose before the preheat and first 0.1s IR_{50} short shine; this second measurement represents a partially bleached status.

This full experiment was repeated for each aliquot using green LEDs instead of blue, and subsequently IR LEDs. Cycles of repeated 0.1s IRSL at 50°C following the same dose and preheat for each aliquot were used to correct the IR_{50} short shine data for signal loss during these measurements (although the results appear very similar even if uncorrected).

In order to explore variability of the bleach form and rate of K feldspar single grains from samples collected in active river channels, bleaching of the MET-IRSL signals using several different protocols have been used. Over the past six years, samples from many different locations including California, USA, Brazil and the UK have been studied; in this paper we focus on behaviour observed using samples collected from a small Scottish River, the Allt Dubhaig, and from the Solimões River, one of the main strands of the Amazon system. The hydrology and sediment movement of the Allt Dubhaig has been extensively studied over several decades (e.g. Ferguson and Ashworth, 1991). With samples from both rivers we observed variability in single grain bleaching parameters using a sequence of blue LED bleaching (51°C, 90% power) within the Risø reader after determination of apparent age for each grain, using a full MET-IRSL SAR protocol (Fig. 1). Using a similar measurement protocol, SAR cycles using a fixed dose of 32 Gy were followed by blue OSL bleach treatments of at half order of magnitude exposure periods (0, 1, 3.2, 10, 32, 100, 320, 1000, 3200, 10,000, 32,000s) prior to the preheat and rest of the SAR cycle for sample 18031 (Allt Dubhaig). A similar treatment was used for sample L0620s (Solimões River) but using a METx-IRSL protocol, and including additional blue LED bleach steps at 0.1, 0.32 and 100,000s.

Two hundred grains from another Allt Dubhaig sample (22183) were used as the basis of a "recovered bleach" experiment. After measuring their natural signals and growth characteristics using a protocol with reduced number of SAR cycles (three for growth, four for bleaching), we quantified the bleaching parameters and their uncertainties for each grain. We then reset the IRSL signals with an ILT-3ET hot bleach (Table 1), dosed them with 51Gy, then exposed them to 32s of blue LEDs (51°C, 90% power). We then started a new SAR cycle with no dose, as if it were a natural cycle measurement using the same protocol, in order to explore the optimum way to match the "recovered bleach" treatment (32s blue LEDs) to the quantified bleach parameters.

4. Results

4.1. Bleaching behaviour

The results of bleaching of the five METx signals using MG aliquots with blue, green and infra-red light at 51°C are displayed in Figure 2 (plots a, b, c) for K feldspar sample MJ39.
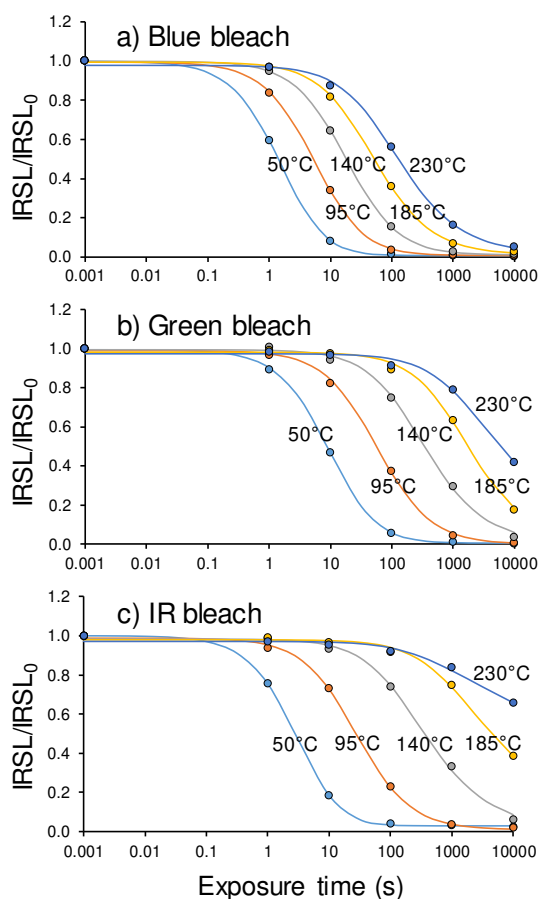

Figure 2. Bleaching of METx-IRSL signals by three different stimulation sources (a: blue, b: green, c: infra-red) using LEDs at 51°C within a RisøTL-DA-20 DASH reader for an orthoclase K-feldspar sample (MJ39) using conventional multiple grain aliquots. See text for further details.

Similar measurements were made using a bytownite plagioclase sample MJ40 (Supplementary Material Figure S1 plots d, e, f); we note absence of a measureable IR-230 signal for the plagioclase sample. For the K-feldspar sample, the blue LED treatment reduces even the hardest-to-bleach METx-IRSL signal at 230°C to a few percent of the initial intensity (shown in these plots at 0.001s for convenience). Each subsequent METx signal is 45°C above the last, and using blue LEDs (plot a), the bleaching rate at 51°C is about half an order of magnitude slower at each different temperature. Lines in Fig. 2 represent least squares fits of the equation of Bailiff & Barnett (1994):

$$I = I_0 / (1 + a.t)^p + c$$

Eq.1

where I is intensity, I_0 is initial intensity, a is bleach rate, p is order of the process, and c represents an unbleachable residual that can account for very slowly bleaching components.

For the K-feldspar sample, bleaching with green LEDs is considerably slower, and each subsequent METx signal is almost an order of magnitude slower (plot b). Bleaching with IR diodes is more effective than green light for the 50°C and 95°C METx signals (plot c), but less rapid for the subsequent temperatures; following 10,000s the 230°C signal is reduced only to around 70% of its initial value.

In contrast, the bytownite plagioclase sample (Fig. S1, plots d, e, f) shows much more rapid 51°C bleaching at all stimulation wavelengths applied, and also much less variation in

bleaching rate for the five different METx-IRSL signals; no significant signal was observed at 230°C, and in each case, the 185°C signal appears to cross the 140°C signal.

4.2. Short shine bleaching determinations

Short shine measurements, described above (sections 3.1, 3.2) were used to explore how the bleaching of the IR_{50} signal by different light sources was affected by the size of the dose administered. Using a wide range of samples, including the lab standard samples described above, no systematic variation in their bleaching form and rate was observed within each sample (although significant differences were seen between samples). This finding was consistent for bleaching by blue, green or IR LEDs, and is also consistent with observations of other MET IRSL signals measured by regular IRSL (i.e. not using short shines). We term a bleach undertaken in these circumstances, that is, with no bleaching since it was last reset by complete zeroing or saturation of that signal, an equilibrium bleach.
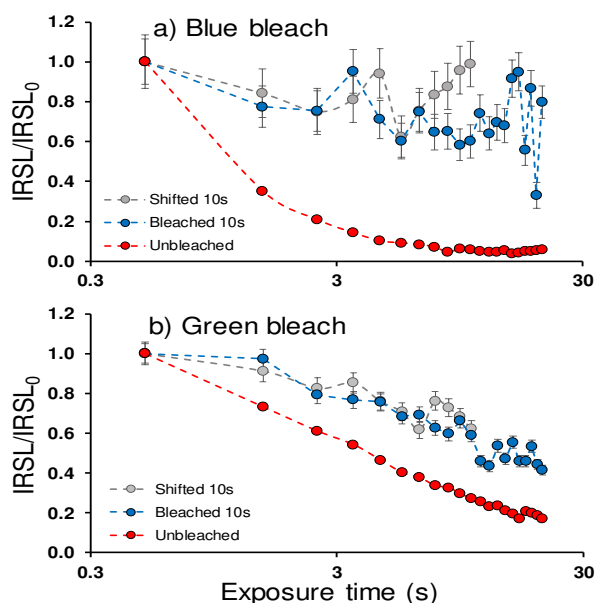

Figure 3. Short shine IRSL data (0.1s at 90% power) for the 50°C signal undergoing repeated bleaching by blue or green light from LEDs within a Risø DASH unit (90% power) normalised to an initial intensity of 1.0. The upper plot (a) shows bleaching by blue LEDs, the lower plot (b) by green LEDs. Measurements without prior bleaching (unbleached) are shown in red, while those shown in blue (bleached 10s) were preceded by a 10s blue light (a) or green light (b) exposure before the initial preheat. The data in grey (shifted 10s) represent the same data as that shown in red on the same plot (unbleached), simply shifted left by 10s on the x-axis to simulate prior bleaching. Note the striking similarity between bleached (blue) and shifted (grey) data points.

In sharp contrast to this, when a sample has been subject to previous partial bleaching, the shape of its subsequent bleaching response is significantly affected. This is illustrated in Fig. 3, where bleaching by blue light (plot a) of a dosed but unbleached aliquot (symbols in red, lowermost data), is compared to the response of the same aliquot given an identical dose, then a 10s blue LED exposure before preheating (blue symbols; see section 3.2 for experimental design) and the unbleached data shifted on the x-axis (time) by 10s (grey symbols). Fig. 3b shows a similar experiment with the same aliquot using bleaching by green LEDs, with (blue

symbols) and without (red symbols) 10s prior green LED exposure, and with the unbleached data shifted by 10s (grey symbols). Note that all data are shown normalized to an initial IRSL intensity of 1.0 to highlight the difference in shape. In the case of the unbleached data translated by 10s and re-normalized (grey symbols), the 10.5s data point in each case is shown at 0.5s with an intensity of 1.0. Similar data were collected for IR bleaching; these are very similar to the green light bleaching data, so these are not displayed here. Bleaching of samples or grains that have previously been partially bleached since their last full resetting, and so decay at a reduced rate as illustrated in Fig. 3, is termed a disequilibrium bleach.

4.3 Natural variations in bleaching rate and form

Blue bleach experiments were undertaken for the MET-IRSL signals of 200 single grains from Allt Dubhaig (sample 18031) using a rigorous 11 point bleaching protocol. The equilibrium decay forms of each response with net initial sensitivity of 1000 counts or more were quantified for the 50 and 95°C signals, and display a surprising degree of variety. High variance in the decay parameters a and p (Eq. 1) was observed, and also in the bleach time to 50% of the initial signal, $t_{50\%}$. For the 50°C signal, these bleach times ($t_{50\%}$) ranged from 1.8 to 34.5s (mean value 8.3 ± 5.5 s), and for the 95°C signal $t_{50\%}$ ranged from 13.2 to 595s (mean value 92.1 ± 111.0 s). We have also explored other samples in this manner, including a sample from the Solimões River Brazil (L0620s), and find similarly wide variation in bleaching parameters, with mean $t_{50\%}$ bleach times of 14.3 ± 14.2s for METx-IR$_{50}$ and 189 ± 199s for METx-IR$_{95}$.

4.4 Recovered bleach experiment

Single grains of sample L0620s from the Solimões River were measured to determine growth and following this, blue LED bleach response after repeated doses; by removing one of the bleaching response data points we are able to assess the variations between grains and at different temperatures in using fitted parameters to recover the exposure time at the missing data point. Data from both the sums of signals from grains on each single grain disc, and from single grains were inspected; several plots are included in the Supplementary Information file. Recovered values were mostly consistent within uncertainties estimated from counting statistics and fitting errors.

Results of the recovered bleach experiments for Allt Dubhaig sample 22183, using an ILT-3ET protocol optimized for measurement speed, are shown in Figure 4. The left hand plots (a, c, e) represent recovered bleach time for grains with measureable signals reconstructed
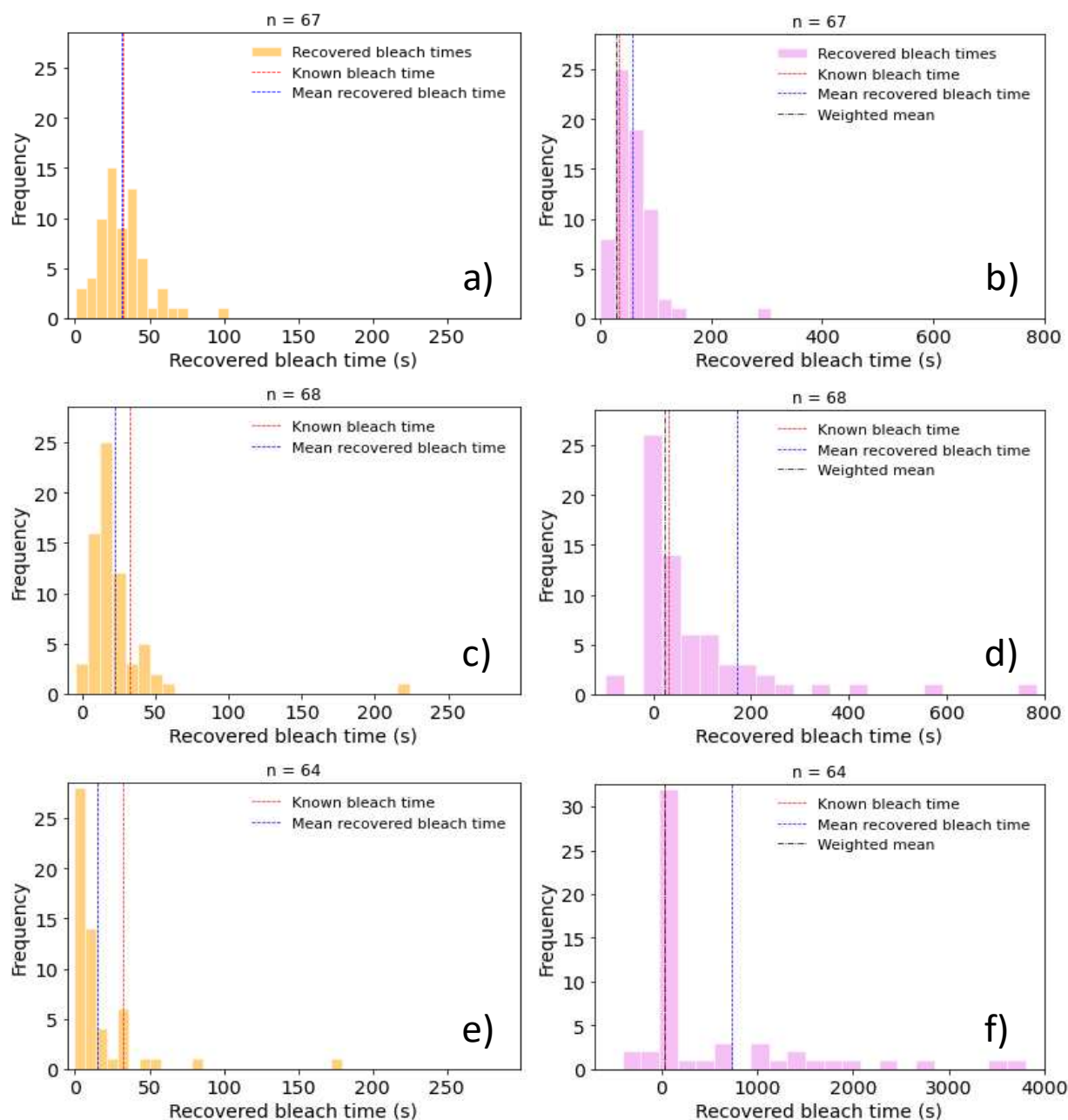
Figure 4. Results of a "bleach recovery" experiment using 200 K-feldspar single grains from the Allt Dubhaig, Perth and Kinross, Scotland, UK. Grains were initially measured using a cut down three point growth and four point blue LED bleach for each grain and an ILT-3ET protocol (see Table 1 for details), then subsequently dosed (57 Gy), bleached using 32s of blue LED exposure, preheated, and the remaining 3ET IRSL signals at 50°C (plots a, b), 95°C (plots c, d), and 140°C (plots e, f) measured. The left hand plots (a, c, e) represent recovered bleach time for grains with measureable signals reconstructed using the average bleach fitting parameters (a, p, c; eq. 1). Data in plots b, d, f on the right show recovered bleach times using bleach fitting parameters determined for each individual grain, along with the unweighted and weighted means of these values. Note that the high dispersion is caused primarily by grains with low bleach parameter precision, and that for each 3ET temperature, the weighted mean values (black dashed lines) in plots b, d, f are close to the given bleach time of 32s.

using the average bleach fitting parameters (a, p, c; eq. 1). Data in plots b, d, f on the right show recovered bleach times using bleach fitting parameters determined for each individual grain, along with the unweighted and weighted means of these values.

Note that the high dispersion in the right hand plots in Fig. 4 is caused primarily by grains with low bleach parameter precision, and that for each 3ET temperature, the weighted mean values (black dashed lines) in plots b, d, f are close to the given bleach time of 32s. The data presented demonstrate successful bleach recovery using different analysis approaches, despite using a reduced measurement protocol.

4.5. Burial bleach model development

In order to reconstruct past behaviour of individual grains, a numerical model of growth and bleaching was constructed. Individual grains may be simulated, as can aliquots or samples, using data from 3ET or MET-IRSL measurements similar to those used in the recovered bleach experiment described above. Signal growth uses an independent saturating exponential function for each IRSL signal, with parameters D_0 and I_{max} derived directly from measurements. Blue LED bleaching is used to determine equilibrium bleach parameters (see equation 1). It is important to note that within the burial-bleach model, as a simulated sample is bleached, subsequent bleaching of that charge population will occur at a reduced bleaching rate (non-equilibrium bleaching), even following a dose treatment. Note, however, that the IRSL signals that derive from the newly acquired trapped charge population that results from this dose (i.e. some fraction of the total trapped charge population responsible for the IRSL signal at this temperature) will bleach, when first exposed to light, with an equilibrium bleach (as this decay shape is always followed irrespective of the size of the dose). For this reason, it is necessary to model these two components (already bleached charge population, newly acquired unbleached charge population) separately with respect to their separate bleaching, though not for their growth. This approach requires accounting for each bleached and dosed component independently, leading to a high degree of complexity when multiple burial-bleach cycles are simulated. Using a model constructed in Python (version 3.11), and validated using manual calculations in spreadsheets, simulations of multiple MET-IRSL signals through many cycles can be achieved, as shown in Figure 5.
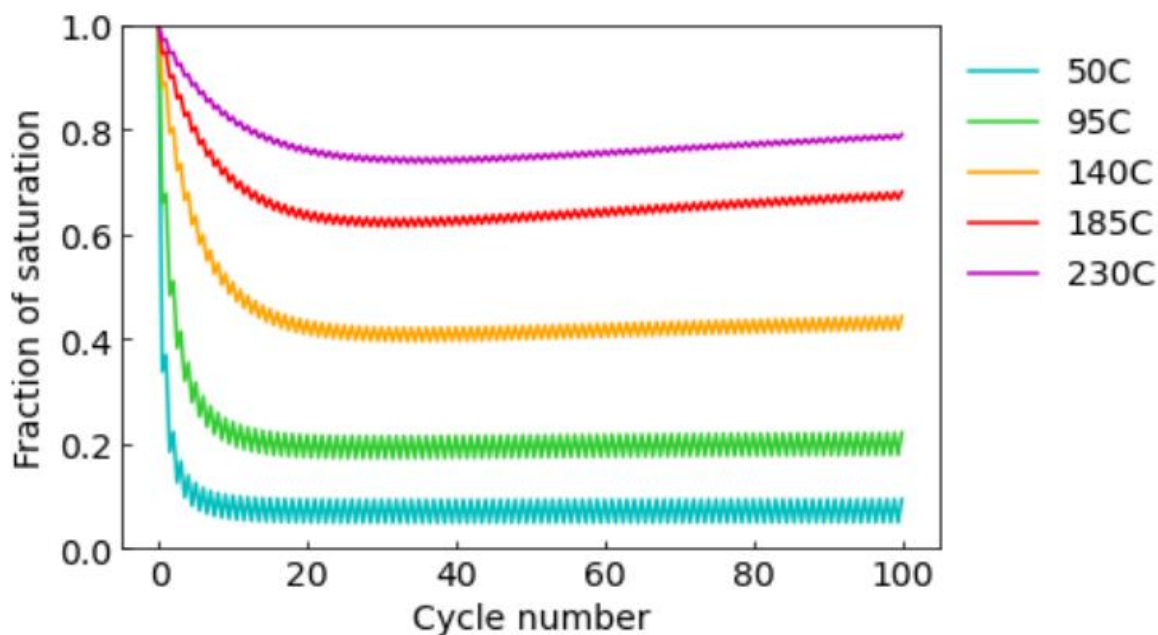
Figure 5. Results of a MET-IRSL burial-bleach model based on numerical simulation using growth and bleach parameters measured for K feldspar laboratory standard MJ39 from California. Model conditions were initial fraction of saturation (FoS) = 1 for all signals, 100 cycles, each with 2s bleach (blue light equivalent) followed by 3000 years of burial. Note the rich behavior of the higher temperature signals as a result of significant non-equilibrium bleach conditions after around 10 cycles, and the effects of saturation as the FoS approaches 1.

5. Discussion

5.1 Bleaching - wavelength and mineral composition

The bleaching curves shown in Fig. 2 demonstrate a good degree of regularity in the removal of charge by light from this K-feldspar standard sample MJ39. However, the three different light sources (blue, green and IR diodes) display different relative bleaching efficiencies for the five MET-IRSL signals.

Bleaching by ambient daylight in natural environments can be highly varied in terms of light intensity, and water depth has significant impact on transmitted wavelengths (Berger and Lauternauer 1987). Dominantly green to amber light is transmitted at depth, though this is heavily attenuated in intensity. In most cases, we are unable to reconstruct ancient bleaching conditions sufficiently to discuss absolute bleaching duration reliably; it appears sensible instead to consider "equivalent bleach time", as used by McGuire and Rhodes (2015a). That study used natural sunlight exposure close to sea level at 34°N to quantify bleaching for the five MET-IRSL signals shown in Fig. 1. using a MG measurement protocol similar to that shown in Table 1 column 3, but with adjusted MG IRSL measurement times.

15

The plagioclase sample used to explore bleaching dependence on feldspar mineral composition is not typical of grains likely to be selected for luminescence measurement. It is composed on bytownite, close to the Ca-rich end member of the plagioclase solid solution series. The very different bleaching behaviour displayed in Figure S1 demonstrates one of the challenges of constructing meaningful numerical simulations of growth and bleaching for grains undergoing sediment transport; grains of different mineral composition are expected to be bleached at different rates under identical environmental conditions. Variation in bleaching behaviour observed for single grains of several samples confirms this high degree of natural variability (section 4.3). Interpretation of observations of SG or MG data with regard to bleaching needs to take this variability into account.

5.2 Prior bleaching

All plots in Fig. 3 show a very clear reduction in decay rate for the previously bleached data (upper symbols), and demonstrate that the prior bleached then preheated data (blue symbols) are almost indistinguishable from the time-shifted data (grey symbols). Note the difference in decay rate shown by the green bleach data (b) is less than shown for the blue bleach data as 10s of green light bleaching reduces the signal less than 10s of blue light.

In contrast, previously unbleached short shine and full MET signal bleaching decays are similar in shape whatever magnitude dose is given. For example, comparison between data points for IR bleaching decays measured after dose values of 8, 34 and 144 Gy showed an average dispersion (1 standard deviation) of less than 2% at all points down the decay, and in another experiment blue LED bleach responses for the five different MET-IRSL signals were indistinguishable in form and rate at dose values of 64, 144 and 576 Gy. In other words, decays measured following different sized dose values are incredibly consistent in terms of bleaching parameters, demonstrating the validity of the concept of an equilibrium bleach.

In summary, when samples have been bleached in the past (since they were last fully bleached and then dosed, or were saturated), the shapes of the MET-IRSL decays on bleaching by all wavelengths tested are changed significantly, here termed non-equilibrium bleaching. However, signals resulting from a dose, irrespective of the size of that dose, have a reproducible bleaching decay form for that sample, aliquot or grain (equilibrium bleaching). These findings have a significant impact in the construction of a burial-bleach numerical model.

Perhaps the most important concept for the reconstruction of multiple cycles of burial and bleaching is referred to as "equilibrium bleaching" of different MET-IRSL signals. This is defined, for the purpose of this publication, as a light exposure following either saturation of the signals involved, or full zeroing followed by growth (in response to dose) without further periods of light exposure. What characterizes this condition is that the bleaching pattern for each signal represents a well-defined form, being that measured following "resetting" by an optical, thermal, or thermo-optical treatment and given a subsequent dose of any magnitude (Fig. 3). Alternatively, saturation can be used to "reset" an IRSL signal to this equilibrium condition.

When a grain undergoes equilibrium bleaching, the form (and rate) of bleaching is predictable and reproducible, at least at a first order level; bleaching decay shape at different dose values does not depart more than a few percent from a standard form. Each signal will decay from an initial value to a value consistent with the bleaching exposure time. In contrast, the form (and rates) of signal bleaching will differ (and specifically, decay will be slower) when in a "non-equilibrium" state. This state is developed by cycles of growth and bleaching that are incomplete; that is, growth that does not take the signal into full saturation, and incomplete or partial bleaching leaves the signal at a level significantly above zero.

Note, we do not expect bleaching forms and rates to be uniform for different grains, but simply remain uniform for different measurements of the same grain when under equilibrium growth conditions. An equilibrium condition is imposed by the hot bleach at the end of each MET-IRSL SAR cycle.

The consequences of non-equilibrium bleaching are that signal reduction rate of all MET-IRSL components is reduced if a bleach event (such as grain exposure during sediment transport) was preceded by additional bleaching. This condition is expected to be almost ubiquitous in sedimentary environments where grains are being actively transported. Incidentally, this may help account for the apparent success in SG-IRSL dating of sediments in relatively mountainous or "raw" environments if bleaching in these contexts is more complete than might be expected based on observations of IRSL in lowland locations (Stokes, 1992).

The "power" of MET-IRSL as a technique to assess grain storage and transport comes from the identification of non-equilibrium states highlighted by non-equilibrium ratios between pairs (or sets) of signals. Further, the degree of disequilibrium can be assessed, and a subset of possible grain history scenarios constrained; with multiple signals, greater constraint is provided, better defining the complex history of cycles of burial and bleaching

by light exposure during transport. For individual grains, a high degree of variability in characteristics is observed, further increasing the depth of data recovery.

5.3 Single grain analysis

An additional power offered by the use of single grains is that a grain is the fundamental unit of sediment transport and history. All parts of a grain can be considered to have shared the same thermal, dose and light exposure history. Different regions within a single grain may have widely varied characteristics (e.g. concentration of traps or luminescence centres, or competitor traps), so the measured single grain luminescence signals still represents the sum of light emission contributions from these zones. However, the responses of different signals from an individual grain cannot vary as a result of differing past conditions (at the scale considered here).

The wide degree of variation in bleaching parameters for single grains mirrors the range of other characteristics that have been observed such as IRSL sensitivity, or growth characteristics. The challenge for sediment transport models is to recognise and make use of this variability, and not to make assumptions that lead to inaccurate conclusions.

The IRSL decay form for each grain, besides control from intrinsic internal characteristics such as the arrangement of lattice defects, geochemical composition and structural controls including grain shape, surface texture and light transmission, may also be affected by external factors such as residual grain coatings. During measurement, the exact position of the IR laser beam relative to each grain can vary, both between grains, but also for the same grain across different SAR cycles. However, beyond this, it seems likely that the same, or similar factors that affect the form of the blue or green light bleaching decay (e.g. Fig. 2) affect the IRSL signal during the measurement. If so, there exists the possibility to derive information about past bleaching and burial history directly from the form of the observed IRSL shine-down measurements; so far, we have not explored this possibility.

5.4 Bleach recovery experiment

We observe significant success from our bleach recovery experiments. In principle, having constructed a bleach response curve, for a given intensity, the corresponding bleach time can be determined using the fitted function (Eq. 1); this can be considered similar to using a growth curve to determine a recovered dose. Using the single grain light sums ("sum all grains") for sample L0602s from Brazil, we observe that the 50° and 95°C recovered bleach

estimates agree very closely with the actual value, but at the higher MET temperatures (140°, 185° and 230°C) the values are slightly over-estimated, though consistent with estimated uncertainties. This appears to be related in part to the smaller signal decreases observed at the 32s bleach point for these higher temperature IRSL data.

The individual grain recovered bleach values for these same measurements of sample L0620s demonstrate a limitation of this approach for some samples, low signal intensity. Despite being able to fit blue LED bleach decay functions to 34 grains at 50°C, and around 20 at each of the higher MET-IRSL temperatures, fewer grains provided the recovered bleach times with useful precision. In other words, few grains provided sufficiently intense signals for the MET-IRSL signals above 50°C to determine bleach times in a useful manner. This also renders our conclusions concerning best approaches for the determination of single grain bleaching characteristics somewhat provisional. We do, however, witness a wide variety of single grain blue bleach responses (figures included in Supplementary file). The recovered bleach times (for a 32s treatment) for the lower three temperatures (50, 95 and 140°C) are, respectively 31.3 ± 3.0s, 43.5 ± 7.1s and 39.9 ± 11.6s based on unweighted mean values.

We observe a significant degree of variation in decay rate and pattern for different single grains from sample L0620s. However, quantifying this variation is impacted by trade-offs between parameters a and p in our fitting (Eq. 1); a similar effect was noted by McGuire and Rhodes (2015a, b). This gives rise to artificially large apparent variance in fitting parameters.

The recovered bleach experiment using sample 22183 from the Allt Dubhaig with a reduced ILT-3ET protocol designed to minimise measurement time was surprisingly successful. The 50°C and 140°C recovered bleach values using individual decays weighted by measurement precision are very close to the given value (29.4 ± 1.6s and 32.5 ± 2.1s respectively). The 95°C value using the same approach underestimates the correct value (22.0 ± 1.4s is recovered versus 32s given bleach time); this appears to be caused by a misfit of one of the more sensitive grains. Using the average bleach time determined for each grain using average fitting parameter values works well at 50°C though with large uncertainty (31.5 ± 17s), but underestimates at higher temperatures, though not outside the large uncertainties. Using an unweighted average of the bleach time using individual decay parameters simply has too much variability; values are within uncertainty limits, but these are greater than 100% for 95° and 140°C data.

Considering the single grain data from these different experiments, it is clear that for sensitive grains, measuring individual bleach parameters has the potential to be successful.

For less sensitive grains, an approach that conjoins individual measurements with combined data (summed or averaged) appears to be the best approach to explore in the future.

5.5 Burial-Bleach model construction

An understanding of the patterns of growth and bleaching experienced by feldspar acquired through the experiments described above, and from many previous studies, has allowed the construction of a burial-bleach model based on numerical simulations of trapped charge populations, using simple differential equations. The model can be used to simulate behaviour at a range of scales, from single grains to aliquots or even samples.

The simulations shown in Fig. 5 illustrate how even under steady state bleaching and growth, in this case repeated cycles of 2s blue light bleaching equivalent exposure and 3,000 years burial (using a dose rate of 3.5 mGya^{-1} based on in-situ NaI gamma spectrometer measurements at the Allt Dubhaig), the behaviour of different MET signals, and the ratios between them can follow unexpected paths as a result of significant non-equilibrium bleaching. For example, note how the 185°C and 230°C signals in Fig. 5 at first fall from an initially saturated conditions, but with subsequent bleach cycles, the rate of bleaching falls so that growth during burial becomes more important. The model does not specifically include the effects of changing trapping competition, beyond use of the measured exponential growth function and measured blue LED bleaching form.

Measurements of growth and bleaching characteristics are required to tune the model for the desired application. The first steps in validating the model were made through the recovered bleach experiment presented above. Further work is required to explore how the model can be used to best effect for the quantification of sediment transport at the single grain level. In principle, a burial-bleach model as described above can be used as a forward model to reconstruct possible signal evolution, but it may also be inverted to match the specific apparent age estimates derived for each MET-IRSL signal of an observed grain.

The key findings presented in this paper are those of equilibrium and disequilibrium bleaching. In some ways it seem remarkable that the form and rate of decay of a feldspar aliquot (or grain) remain indistinguishable over a very wide range of applied dose, so long as that aliquot has not been bleached since its last resetting event. In the authors' understanding, resetting includes signal zeroing by light, heat, or a combination of these, or by dose saturation of the signals involved.

6. Conclusions

MET-IRSL, and the simplified protocol of 3ET, have the potential to provide significant information about past bleaching events even at the scale of individual grains of feldspar, along with burial histories. This provides the potential for deriving information about sediment transport and storage at the single grain level. The remarkable consistency of equilibrium bleaching within each sample is a surprising and important discovery, while non-equilibrium bleaching following prior exposure is important to the construction of reliable burial-bleach simulations. A bleach recovery experiment was successful, and highlights further opportunities to develop improved means for combining average or summed data with individual measurements.

References

Bailiff, I.K., Barnett, S.M., 1994. Characteristics of infrared stimulated luminescence from a feldspar at low temperatures. Radiation Measurements 23, 541–546.

Berger, G.W., Lauternauer, J.J., 1987, Preliminary field work for thermoluminescence dating studies at the Fraser River delta, British Columbia. Geological Survey of Canada paper 87-1A, 901-904.

Colls, A.E., Stokes, S., Blum, M.D., Straffin, E., 2001, Age limits on the Late Quaternary evolution of the upper Loire River. Quaternary Science Reviews 20, 743-750.

Daniels, J.T.M., (2016). Mineralogic controls on the infrared stimulated luminescence of feldspars: an exploratory study of the effects of Al,Si order and composition on the behavior of a modified post-IR IRSL signal. Unpublished MS thesis, University of California, Los Angeles.

Fu, X., Li, S.H., 2013. A modified multi-elevated-temperature post-IR IRSL protocol for dating Holocene sediments using K-feldspar. Quat. Geochronol. 17, 44–54.

Ferguson, R. and Ashworth, P., 1991. Slope-induced changes in channel character along a gravel-bed stream: the Allt Dubhaig, Scotland. Earth Surface Processes and Landforms, *16*(1), pp.65-82.

Gemmell, A.M.D., 1985. Zeroing of the TL signal of sediment undergoing fluvial transportation: a laboratory experiment. Nuclear Tracks and Radiation Measurements 10, 695-702.

Gemmel, A.M.D., 1988. Thermoluminescence dating of glacially transported sediments: some considerations. Quaternary Science Reviews 7, 277-285.

Gray, H., Tucker, G.E., Mahan, S., McGuire C., Rhodes, E.J., 2017 On extracting sediment transport information from measurements of luminescence in river sediments. Journal of Geophysical Research-Earth Surface 122, 654–677, doi:10.1002/2016JF003858

Gray, H., Tucker, G. & Mahan, S.,(2018). Application of a Luminescence-Based Sediment Transport Model. Geophysical Research Letters 45, 6071-6080. 10.1029/2018GL078210

Gray, H.J., Jain, M., Sawakuchi, A.O., Mahan, S.A., Tucker, G.E. (2019). Luminescence as a sediment tracer and provenance tool. Reviews of Geophysics 57, https://doi.org/10.1029/2019RG000646

Guerin, G., Visocekas, R., 2015. Volcanic feldspars anomalous fading: evidence for two different mechanisms. Radiation Measurements 79, 1–6.

Guralnik, B., and Sohbati, R. (2019). "Fundamentals of photo- and thermochronometry," in Advances in thermoluminescence and optically stimulated luminescence: Theory, experiments and applications. Editors R. Chen and V. Pagonis (Singapore: World Scientific).

Guyez, A., Bonnet, S., Reimann, T., Carretier, S., & Wallinga, J. (2023). A novel approach to quantify sediment transfer and storage in rivers—testing feldspar single-grain pIRIR analysis and numerical simulations. Journal of Geophysical Research: Earth Surface 128, e2022JF006727. https://doi.org/10.1029/2022JF006727

Huntley, D. J. (2006). An explanation of the power-law decay of luminescence. Journal of Physics: Condensed Matter, 18(4), 1359.

Huntley, D.J., Lamothe, M., 2001. Ubiquity of anomalous fading in K-feldspars and the measurement and correction for it in optical dating. Can. J. Earth Sci. 38, 1093–1106.

Ivester, A.H., Rhodes, E.J., F Dolan, J.F., Van Dissen, R.J., Gauriau, J.,Little, T., McGill, S.F., Tuckett, P.A., 2022 A method to evaluate the degree of bleaching of IRSL signals in

feldspar: The 3 ET method. Quaternary Geochronology 101346, https://doi.org/10.1016/j.qua-geo.2022.101346

Jain, M., Ankjærgaard, C., 2011 Towards a non-fading signal in feldspar: Insight into charge transport and tunnelling from time-resolved optically stimulated luminescence. Radiation Measurements 46, 292-309, doi: 10.1016/j.radmeas.2010.12.004

Jenkin, G.T.H., Duller, G.A.T., Roberts, H.M., Chiverrell, R.C., Glasser, N.F., 2018. A new approach for luminescence dating glaciofluvial deposits – high precision optical dating of cobbles. Quat. Sci. Rev. 192, 263–273.

Kars, R.H., Reimann, T., Wallinga, J., 2014. Are feldspar SAR protocols appropriate for post-IR IRSL dating? Quat. Geochronol. 22, 126-136.

Lapp, T., Kook, M., Murray, A.S., Thomsen, K.J., Buylaert, J.-P., Jain, M., 2015. A new luminescence detection and stimulation head for the Risø TL/OSL reader. Radiat. Meas. 81, 178–184.

Lawson, M.J., Daniels, J.T.M., Rhodes, E.J. 2015 Assessing Optically Stimulated Luminescence (OSL) signal contamination within small aliquots and single grain measurements utilizing the composition test. Quaternary International 362, 34-41, http://dx.doi.org/10.1016/ j.quaint.2014.05.017

Li, B., Jacobs, Z., Roberts, R.G., Li, S.H., 2018. Single-grain dating of potassium-rich feldspar grains: towards a global standardised growth curve for the post-IR IRSL signal. Quat. Geochronol. 45, 23–36.

Li, B., Li, S.H., 2011. Luminescence dating of K-feldspar from sediments: a protocol without anomalous fading correction. Quat. Geochronol. 6, 468–479.

Liu, Q, Chen, J., Qin, J., Yang, H., Di, N., Liu, J., Zhang, W. (2022) MET-post-IR IRSL luminescence dating of cobbles buried in fluvial terraces in the Northern Chinese Tian Shan Quaternary Geochronology 72, 101351, https://doi.org/10.1016/j.quageo.2022.101351

McGuire, C.P., Rhodes, E.J. (2015a). Determining fluvial sediment virtual velocity on the Mojave River using K-feldspar IRSL: Initial assessment. Quaternary International, 362, 124–131.

McGuire, C.P., Rhodes, E.J., (2015b). Downstream MET-IRSL single-grain distributions in the Mojave River, southern California: Testing assumptions of a virtual velocity model. Quaternary Geochronology, 30, 239-244.

Pagonis, V. Mayank Jain, M., Andrew S. Murray, A.S., Christina Ankjærgaard, C., Reuven Chen, R., 2012 Modeling of the shape of infrared stimulated luminescence signals in feldspars. Radiation Measurements 47 (9), 870-876. https://doi.org/10.1016/j.radmeas.2012.02.012.

Pederson, J.L., Chapot, M.S., Simms, S.R., Sohbati, R., Rittenour, T.M., Murray, A.S., Cox, G. 2014. Age of Barrier Canyon-style rock art constrained by cross-cutting relations and luminescence dating techniques. Proceedings of the National Academic of Sciences of the United Stated of America (PNAS) 111 (36), 12986-12991, DOI: 10.1073/pnas.1405402111.

Poolton, N.R.J., Ozanyan, K.B., Wallinga, J., Murray, A.S., Bøtter-Jensen, L., 2002b. Electrons in feldspar II: a consideration of the influence of conduction band-tail states on luminescence processes. Phys. Chem. Minerals 29, 217e225.

Reimann, T., Notenboom, P.D., Schipper, M.A.D., Wallinga, J., 2015. Testing for sufficient signal resetting during sediment transport using a polymineral multiplesignal luminescence approach. Quat. Geochronol. 25, 26–36.

Rhodes, E.J. 2015 Dating sediments using potassium feldspar single-grain IRSL: initial methodological considerations. Quaternary International 362, 14-22 http://dx.doi.org/10.1016/j.quaint.2014.12.012

Rhodes, E.J., Leathard, J.A., 2022 MET-IRSL used to track pre-depositional sediment transport history, Quaternary Geochronology, 101294, https://doi.org/10.1016/j.quageo.2022.101294

Rhodes, E.J., Walker, R.T. 2019 Applications of luminescence dating to active tectonic contexts. In: Handbook of luminescence dating (Bateman, M.D. ed.). Whittles publishing, Caithness, 293-320.

Sohbati, R., Murray, A.S., Chapot, M.S., Jain, M., Pederson, J., (2012). Optically stimulated luminescence (OSL) as a chronometer for surface exposure dating. J. Geophys. Res.117, B09202. https://doi .org /10 .1029 /2012JB009383.

Stokes, S., 1992. Optical dating of young (modern) sediments using quartz: results from a selection of depositional environments. Quaternary Science Reviews 11, 153-159.

Stokes, S., Bray, H.E., Blum, M.D., 2001. Optical resetting in large drainage basins: tests of zeroing assumptions using single-aliquot procedures. Quaternary Science Reviews 20, 879-885.

Zhang, J., Guralnik, B., Tsukamoto, S., Ankjærgaard, C., Reimann, T., (2023), The bleaching limits of IRSL signals at various stimulation temperatures and their potential inference of the preburial light exposure duration. Front. Earth Sci. 10:933131. doi: 10.3389/feart.2022.933131